Metal–Hydride Bond Activation and Metal–Metal Interaction in Dinuclear Iron Complexes with Linking Dinitriles: A Synthetic, Electrochemical, and Theoretical Study

ARTICLE *in* INORGANIC CHEMISTRY · JANUARY 2003

Impact Factor: 4.76 · DOI: 10.1021/ic025835k · Source: PubMed

6 AUTHORS, INCLUDING:

Maxim L. Kuznetsov
University of Lisbon
105 PUBLICATIONS **1,973** CITATIONS
SEE PROFILE

M Fátima C Guedes da Silva
University of Lisbon
260 PUBLICATIONS **4,155** CITATIONS
SEE PROFILE

Inorg. Chem. **2002**, *41*, 6456–6467

Metal–Hydride Bond Activation and Metal–Metal Interaction in Dinuclear Iron Complexes with Linking Dinitriles: A Synthetic, Electrochemical, and Theoretical Study

Ana I. F. Venâncio,[†] Maxim L. Kuznetsov,[†] M. Fátima C. Guedes da Silva,[†,‡] Luísa M. D. R. S. Martins,[†,§] João J. R. Fraústo da Silva,[†] and Armando J. L. Pombeiro*[,†]

Centro de Química Estrutural, Complexo I, Instituto Superior Técnico, Av. Rovisco Pais, 1049-001 Lisboa, Portugal, Universidade Lusófona de Humanidades e Tecnologias, Campo Grande, 376, 1749-024 Lisboa, Portugal. and Secção de Química Inorgânica, DEQ, ISEL, R. Conselheiro Emídio Navarro, 1949-014 Lisboa, Portugal

Received July 1, 2002

The dinuclear iron(II)–hydride complexes $[\{FeH(dppe)_2\}_2(\mu\text{-LL})][BF_4]_2$ (LL = NCCH=CHCN (**1a**), NCC_6H_4CN (**1b**), $NCCH_2CH_2CN$ (**1c**); dppe = $Ph_2PCH_2CH_2PPh_2$) and the corresponding mononuclear ones, *trans*-$[FeH(LL)(dppe)_2][BF_4]$ (**2a**–**c**) were prepared by treatment of *trans*-$[FeHCl(dppe)_2]$, in tetrahydrofuran (thf) and in the presence of $Tl[BF_4]$, with the appropriate dinitrile (in molar deficiency or excess, respectively). Metal–metal interaction was detected by cyclic voltammetry for **1a**, which, upon single-electron reversible oxidation, forms the mixed valent Fe^{II}/Fe^{III} **1a**$^+$ complex. The latter either undergoes heterolytic Fe–H bond cleavage (loss of H^+) or further oxidation, at a higher potential, also followed by hydride-proton evolution, according to ECECE or EECECEC mechanistic processes, respectively, which were established by digital simulation. Anodically induced Fe–H bond rupture was also observed for the other complexes and the detailed electrochemical behavior, as well as the metal–metal interaction (for **1a**), were rationalized by ab initio calculations for model compounds and oxidized derivatives. These calculations were used to generate the structural parameters (full geometry optimization), the most stable isomeric forms, the ionization potentials, the effective atomic charges, and the molecular orbital diagrams, as well as to predict the nature of the other electron-transfer induced chemical steps, i.e. geometric isomerization and nucleophilic addition, by BF_4^-, to the unsaturated iron center resulting from hydride-proton loss. From the values of the oxidation potential of the complexes, the electrochemical P_L and E_L ligand parameters were also estimated for the dinitrile ligands (LL) and for their mononuclear complexes **2** considered as ligands toward a second binding metal center.

Introduction

Transition metal−hydrogen bonds play a relevant role in coordination chemistry, namely, in laboratorial, industrial, and biological catalyses, and electrochemical methods provide convenient tools for the investigation of their activation by electron transfer (ET). Nevertheless and in contrast with the well-developed hydride chemistry,[1] the electrochemistry of hydride complexes has been barely investigated.[2−10] A versatile reactivity can follow the ET-induced metal−hydrogen bond cleavage but only very rarely have the mechanisms been reported, in all the cases, to the best of

* E-mail: pombeiro@ist.utl.pt.
† Instituto Superior Técnico.
‡ Universidate Lusófona de Humanidades e Tecnologias.
§ DEQ, ISEL.

(1) *Recent Advances in Hydride Chemistry*; Peruzzini, M., Poli, R., Eds.; Elsevier: Amsterdam, 2001.

(2) (a) Tilset, M.; Fjeldahl, I.; Hamon, J. R.; Touplet, L.; Saillard, J. Y.; Costuas, K.; Haynes, A. *J. Am. Chem. Soc.* **2001**, *123*, 9984. (b) Rømming, C.; Smith, K.-T.; Tilset, M. *Inorg. Chim. Acta* **1997**, *259*, 281. (c) Smith, K.-T.; Rømming, C.; Tilset, M. *J. Am. Chem. Soc.* **1993**, *115*, 8681. (d) Andrei, A. Z.; Tilset, M.; Caulton, K. G. *Inorg. Chem.* **1993**, *32*, 3816. (e) Ryan, O. B.; Tilset, M. *J. Am. Chem. Soc.* **1991**, *113*, 9554. (f) Ryan, O. B.; Tilset, M.; Parker, V. D. *Organometallics* **1991**, *10*, 298. (g) Ryan, O. B.; Tilset, M.; Parker, V. D. *J. Am. Chem. Soc.* **1990**, *112*, 2618.

(3) (a) Prenzler, P. D.; Boskovic, C.; Bond, A. M.; Wedd, A. G. *Anal. Chem.* **1999**, *71*, 3650. (b) Monglet, D.; Bond, A. M.; Coutinho, K.; Dickson, R. S.; Lazarev, G. G.; Olsen, S. A.; Pilbrow, J. R. *J. Am. Chem. Soc.* **1998**, *120*, 2086. (c) Marken, F.; Bond, A. M.; Colton, R. *Inorg. Chem.* **1995**, *34*, 1705.

(4) Bianchini, C.; Peruzzini, M.; Ceccante, A.; Laschi, F.; Zanello, P. *Inorg. Chim. Acta* **1997**, *259*, 61.

10.1021/ic025835k CCC: $22.00
Published on Web 10/31/2002

our knowledge, concerning starting mononuclear hydride complexes. Moreover, no theoretical calculations appear to have been applied to the detailed interpretation of the ET-promoted processes in such systems. Hence, the electrochemical investigation of dinuclear dihydride complexes, and the comparison of their behavior with that of the mononuclear hydride constituents, as well as the rationalization of such behaviors by theoretical studies, would be a matter of considerable interest. The possibility of occurrence of a metal−metal interaction via a suitable bridging ligand in the former complexes would constitute a further motif of interest in view of the significance of such interaction for the understanding of the electrochemical, magnetic, spectroscopic, and semiconductor[11a] and nonlinear optical[11b] properties and in the application of such complexes, e.g. in molecular electronics,[12−15] biochemistry,[16−20] multielectron redox reactions of small molecules[21] and as a support to the formation of dendrimers and coordination polymers.[22] The communication between the two metal atoms has been studied with a variety of linkage ligands[22−36] (although dinitriles[36] do not appear to have been fully explored, despite their availability and simplicity) and metals by electrochemical or spectroelectrochemical,[25b−d,26−28,30a,31,32b,d,35b,c,37−41] ESR,[25c,d,26−28,35a,c,41a,42] and other spectroscopic[24,25b−d,27,28,32b,d,35c,38,39,41a] methods and also by theoretical quantum chemical investigations, mainly by Hückel or extended Hückel (EHMO)[23,31,32b,35a,37,43] (but also INDO/1,[39,41a,43] HF[25c,29,44] or DFT[25c,e,j,27,28,30a,33,42,45]) methods.

By taking into consideration the above motives and that we have previously investigated in detail the mechanism of the anodic process of the hydride isocyanide complexes *trans*-$[FeH(CNR)(dppe)_2]^+$ (R = alkyl, aryl; dppe = $Ph_2PCH_2CH_2PPh_2$), which proceeds via the initial ET-induced Fe−H bond cleavage followed by further reactivity, according to a curious ECEC (E = ET step, C = chemical step) reaction mechanism, we decided to prepare and investigate by electrochemical and ab initio methods the following compounds: the dinuclear complexes $[\{FeH(dppe)_2\}_2(\mu\text{-LL})][BF_4]_2$ with the conjugated bridging fumaronitrile (LL = NC−CH═CH−CN, **1a**) or terephthalonitrile (1,4-dicyanobenzene) [LL = NC(1,4-C_6H_4)NC, **1b**] ligands or with the

(5) Berning, D. E.; Noll, B. C.; Dubois, D. L. *J. Am. Chem. Soc.* **1999**, *121*, 11432.
(6) Westerberg, D. E.; Rhodes, L. F.; Edwin, J.; Geiger, W. E.; Caulton, K. G. *Inorg. Chem.* **1991**, *30*, 1107.
(7) Klingler, R. J.; Huffman, J. C.; Kochi, J. K. *J. Am. Chem. Soc.* **1980**, *102*, 208.
(8) Almeida, S. S. P. R.; Guedes da Silva, M. F. C.; Fraústo da Silva, J. J. R.; Pombeiro, A. J. L., *J. Chem. Soc., Dalton Trans*. **1999**, 467.
(9) (a) Lemos, M. A. N. D. A.; Pombeiro, A. J. L. *J. Organomet. Chem.* **1992**, *438*, 159. (b) Lemos, M. A. N. D. A.; Pombeiro, A. J. L. *J. Organomet. Chem.* **1987**, *332*, C17.
(10) Amatore, C.; Fraústo da Silva, J. J. R.; Guedes da Silva, M. F. C.; Pombeiro, A. J. L.; Verpeaux, J.-N. *J. Chem. Soc., Chem. Commun.* **1992**, 1289.
(11) (a) DeRosa, M. C.; Al-mutlaq, F.; Crutchley, R. J. *Inorg. Chem.* **2001**, *40*, 1406, and references therein. (b) Ferretti, A.; Lami, A.; Villani, G. J. *J. Phys. Chem.* **1997**, *101*, 9439.
(12) Astruc, D. *Acc. Chem. Res.* **1997**, *30*, 383, and references therein.
(13) Mikkelsen, K. V.; Ratner, M. A. *Chem. Rev.* **1987**, *87*, 113.
(14) McCleverty, J. A.; Ward, M. D. *Acc. Chem. Res.* **1998**, *31*, 842.
(15) Astruc, D. *Electron Transfer and Radical Processes in Transition-Metal Chemistry*; VCH: New York, 1995.
(16) Solomon, E. I.; Brunold, T. C.; Davis, M. I.; Kemsley, J. N.; Lee, S.-K.; Lehnert, N.; Neese, F.; Skulan, A. J.; Yang, Y.-S.; Zhou, J. *Chem. Rev.* **2000**, *100*, 235.
(17) Blondin, G.; Girerd, J.-J. *Chem. Rev.* **1990**, *90*, 1359.
(18) Marcus, R. A.; Sutin, N. *Biochim. Biophys. Acta* **1985**, *811*, 265.
(19) Beratan, D. N.; Betts, J. N.; Onuchic, J. N. *Science* **1991**, *252*, 1285.
(20) Bominaar, E. L.; Achim, C.; Borshch, S. A.; Gired, J.-J.; Münck, E. *Inorg. Chem.* **1997**, *36*, 3689.
(21) Nishida, Y.; Shimo, H.; Maehara, H.; Kida, S. *J. Chem. Soc., Dalton Trans.* **1985**, 1945.
(22) (a) Balzani, V.; Campagna, S.; Denti, G.; Juris, A.; Serroni, S.; Venturi, M. *Acc. Chem. Res.* **1998**, *31*, 26. (b) Bodige, S.; Torres, A. S.; Maloney, D. J.; Tate, D.; Kinsel, G. R.; Walker, A. K.; MacDonnell, F. M. *J. Am. Chem. Soc.* **1997**, *119*, 10364. (c) Neels, A.; Neels, B. M.; Stoeckli-Evans, H.; Clearfield, A.; Poojary, D. M. *Inorg. Chem.* **1997**, *36*, 3402.
(23) Kaim, W.; Klein, A.; Glöckle, M. *Acc. Chem. Res.* **2000**, *33*, 755, and references therein.
(24) Creutz, C.; Taube, H. *J. Am. Chem. Soc.* **1973**, *95*, 1086.
(25) (a) Lay, P. A.; Magnuson, R. H.; Taube, H. *Inorg. Chem.* **1988**, *27*, 2364. (b) Bruns, W.; Kaim, W.; Waldhör, E.; Krejcik, M. *Inorg. Chem.* **1995**, *34*, 663. (c) Klein, A.; Kasack, V.; Reinhardt, R.; Sixt, T.; Scheiring, T.; Zalis, S.; Fiedler, J.; Kaim, W. *J. Chem. Soc., Dalton Trans.* **1999**, 575. (d) Ketterle, M.; Kaim, W.; Olabe, J. A.; Parise, A. R.; Fiedler, J. *Inorg. Chim. Acta* **1999**, *291*, 66. (e) Bencini, A.; Ciofini, I.; Daul, C. A.; Ferretti, A. *J. Am. Chem. Soc.* **1999**, *121*, 11418.
(26) Das, A.; Maher, J. P.; McCleverty, J. A.; Navas Badiola, J. A.; Ward, M. D. *J. Chem. Soc., Dalton Trans.* **1993**, 681.
(27) Klein, A.; Kaim, W.; Hornung, F. M.; Fiedler, J.; Zalis, S. *Inorg. Chim. Acta* **1997**, *264*, 269.
(28) Glöckle, M.; Kaim, W.; Klein, A.; Roduner, E.; Hübner, G.; Zalis, S.; van Slageren, J.; Renz, F.; Gütlich, P. *Inorg. Chem.* **2001**, *40*, 2256.
(29) Mosher, P. J.; Yap, G. P. A.; Crutchley, R. J. *Inorg. Chem.* **2001**, *40*, 1189.
(30) (a) Hogarth, G.; Humphrey, D. G.; Kaltsoyannis, N.; Kim, W.-S.; Lee, M.; Norman, T.; Redmond, S. P. *J. Chem. Soc., Dalton Trans.* **1999**, 2705. (b) Antiñolo, A.; Carrillo-Hermosilla, F.; Otero, A.; Fajardo, M.; Garcés, A.; Gómez-Sal, P.; López-Mardomingo, C.; Martin, A.; Miranda, C. *J. Chem. Soc., Dalton Trans.* **1998**, 59.
(31) Alias, Y.; Abasq, M.-L.; Barrière, F.; Davies, S. C.; Fairhurst, S. A.; Hughes, D. L.; Ibrahim, S. K.; Talarmin, J.; Pickett, C. J. *J. Chem. Soc., Chem. Commun.* **1998**, 675.
(32) (a) Brady, M.; Weng, W.; Zhou, Y.; Seyler, J.; Amaroso, A. J.; Arif, A. M.; Böhme, M.; Frenking, G.; Gladysz, J. A. *J. Am. Chem. Soc.* **1997**, *119*, 775. (b) Brady, M.; Weng, W.; Gladysz, J. A. *J. Chem. Soc., Chem. Commun.* **1994**, 2655. (c) Le Narvor, N.; Toupet, L.; Lapinte, C. *J. Am. Chem. Soc.* **1995**, *117*, 7129. (d) Passaniti, P.; Browne, W. R.; Lynch, F. C.; Hughes, D.; Nieuwenhuyzen, M.; James, P.; Maestri, M.; Vos, J. G. *J. Chem. Soc., Dalton Trans.* **2002**, 1740.
(33) Unseld, D.; Krivykh, V. V.; Heinze, K.; Wild, F.; Artus, G.; Schmalle, H.; Berke, H. *Organometallics* **1999**, *18*, 1525.
(34) (a) Shih, K.-Y.; Schrock, R. R.; Kempe, J. *J. Am. Chem. Soc.* **1994**, *116*, 8804. (b) Woodworth, B. E.; White, P. S.; Templeton, J. L. *J. Am. Chem. Soc.* **1997**, *119*, 828.
(35) (a) Colin, J. C.; Mallah, T.; Journaux, Y.; Lloret, F.; Julve, M.; Bois, C. *Inorg. Chem.* **1996**, *35*, 4170. (b) McQuillan, F. S.; Berridge, T. E.; Chen, H.; Hamor, T. A.; Jones, C. J. *Inorg. Chem.* **1998**, *37*, 4959. (c) Ernst, S.; Hänel, P.; Jordanov, J.; Kaim, W.; Kasack, V.; Roth, E. *J. Am. Chem. Soc.* **1989**, *111*, 1733.
(36) (a) Krentzien, H.; Taube, H. *J. Am. Chem. Soc.* **1976**, *98*, 6379. (b) Richardson, D. E.; Taube, H. *Inorg. Chem.* **1981**, *20*, 1278.
(37) Kaim, W.; Kasack, V. *Inorg. Chem.* **1990**, *29*, 4696.
(38) Joulié, L. F.; Schatz, E.; Ward, M. D.; Weber, F.; Yellowlees, L. J. *J. Chem. Soc., Dalton Trans.* **1994**, 799.
(39) Rocha, R. C.; Araki, K.; Toma, H. E. *Inorg. Chim. Acta* **1999**, *285*, 197.
(40) Bear, J. L.; Han, B.; Wu, Z.; Van Caemelbecke, E.; Kadish, K. M. *Inorg. Chem.* **2001**, *40*, 2275.
(41) (a) Ung, V. Â.; Bardwell, D. A.; Jeffery, J. C.; Maher, J. P.; McCleverty, J. A.; Ward, M. D.; Williamson, A. *Inorg. Chem.* **1996**, *35*, 5290. (b) Ung, V. Â.; Couchman, S. M.; Jeffery, J. C.; McCleverty, J. A.; Ward, M. D.; Totti, F.; Gatteschi, D. *Inorg. Chem.* **1999**, *38*, 365.
(42) Bencini, A.; Daul, C. A.; Dei, A.; Mariotti, F.; Lee, H.; Shultz, D. A.; Sorace, L. *Inorg. Chem.* **2001**, *40*, 1582.
(43) Patoux, C.; Launay, J.-P.; Beley, M.; Chodorowski-Kimmes, S.; Collin, J.-P.; James, S.; Sauvage, J.-P. *J. Am. Chem. Soc.* **1998**, *120*, 3717.
(44) Hart, J. R.; Rappé, A. K.; Gorun, S. M.; Upton, T. H. *Inorg. Chem.* **1992**, *31*, 5254.
(45) Barone, V.; Bencini, A.; Ciofini, I.; Daul, C. A.; Totti, F. *J. Am. Chem. Soc.* **1998**, *120*, 8357.

nonconjugated succinonitrile bridge (LL = NC−CH_2CH_2−CN, **1c**), as well as, for comparative purposes, the corresponding mononuclear compounds [FeH(LL)$(dppe)_2$][BF_4] (**2a**−**c**). The investigation of the activation of the Fe−H bond by ET also constitutes a matter of potential biological significance toward the understanding of the enzymatic action of iron−hydrogenases[46] and nitrogenases.[47] The study also provides an opportunity to extend to dinuclear dinitrile complexes the investigation of the electronic properties, coordinating and activating abilities of N_2-binding iron phosphinic centers which we have been using, in mononuclear complexes, for other small unsaturated substrates such as organosilanes,[8] cyanamides and cyanoguanidine,[48] mononitriles,[49] isocyanides,[8,9,50] phosphaalkynes,[51] and alkynes and carbon disulfide.[52]

Experimental Section

All manipulations and reactions were carried out using standard inert gas flow or high-vacuum techniques. The complex *trans*-[FeHCl$(dppe)_2$] was prepared by a published method;[53] the dinitriles were used as purchased from Aldrich. The solvents were purified and dried by standard methods and freshly distilled under dinitrogen. The IR spectra (400−4000 cm^{-1}) were recorded on a Bio-Rad FTS 3000MX instrument in KBr pellets. NMR spectra (run in CD_2Cl_2 unless stated otherwise) on a Varian UNITY 300 spectrometer at room temperature. ^1H, ^{13}C, $^{13}C\{^1H\}$, and $^{31}P\{^1H\}$ chemical shifts (δ) are reported in parts per million relative to tetramethylsilane (TMS) and H_3PO_4, respectively. In the ^{13}C NMR data, assignments and coupling constants common to the $^{13}C\{^1H\}$ NMR spectra are not reported. Abreviations: s = singlet; d = doublet; t = triplet; q = quartet; qnt = quintet; tqnt = triplet of quintet; m = multiplet. UV/vis spectra were recorded on a Perkin-Elmer Lambda-9 spectrophotometer. The spectral range between 230 and 850 nm was covered by using quartz cells. Results are reported in terms of ϵ (molar adsorption coefficient) in $M^{-1}\cdot cm^{-1}$. C, H, and N elemental analyses were carried out by the Microanalytical Service of the Instituto Superior Técnico. Positive-ion FAB mass spectra were obtained on a Trio 2000 instrument by bombarding 3-nitrobenzyl alcohol matrices of the samples with 8 keV (ca. 1.28×10^{-15} J) Xe atoms. Nominal molecular masses were calculated using the most abundant isotopes ^{56}Fe (52%). However, further complexity due to addition (from the matrix) or loss of hydrogen was usually not taken into account. Mass calibration for data system acquisition was achieved using CsI.

Syntheses. (a) Dinuclear Complexes [{FeH$(dppe)_2$}$_2$(μ-LL)][BF_4]$_2$ (LL = NCCH=CHCN (1a), NCC_6H_4CN (1b), $NCCH_2CH_2CN$ (1c)). These complexes can be obtained either directly from *trans*-[FeHCl$(dppe)_2$] (method A) or, in a less straightforward way, from the corresponding mononuclear complexes **2** (see below; method B).

(1) Method A. A solution of *trans*-[FeHCl$(dppe)_2$] (0.20 g, 0.22 mmol) in tetrahydrofuran (thf) (20 cm^3) was stirred under dinitrogen, at room temperature, for 15−30 min with Tl[BF_4] (0.070 g, 0.25 mmol). The appropriate dinitrile (LL) was then added [0.009 g, 0.11 mmol (NCCH=CHCN); 0.014 g, 0.11 mmol (NCC_6H_4CN); 0.005 g, 0.006 mmol ($NCCH_2CH_2CN$)], and the mixture was stirred at room temperature for ca. 20 h, whereafter it was taken to dryness by evaporation of the solvent in vacuo. Extraction with CH_2Cl_2 (20 cm^3) followed by filtration (removal of the thallium salts), concentration in vacuo to ca. 10 cm^3, and addition of diethyl ether (ca. 5−7 cm^3) led to the precipitation of the dinuclear product as a blue (**1a**), red (**1b**) or yellow (**1c**) solid which was separated by filtration, washed with Et_2O, dried in vacuo, and recrystallized from CH_2Cl_2/Et_2O [0.16 g, 72% yield (**1a**); 0.18 g, 81% yield (**1b**); 0.054 g, 48% yield (**1c**)].

(2) Method B. The above dinuclear complexes **1** can also be obtained by reacting the corresponding mononuclear complexes **2** (see below) with the stoichiometric amount of *trans*-[FeHCl$(dppe)_2$]. As a typical example, the synthesis of **1a** from **2a** is given: A solution of *trans*-[FeHCl$(dppe)_2$] (0.027 g, 0.030 mmol) in thf (10 cm^3) was stirred under dinitrogen, at room temperature, for 15 min in the presence of Tl[BF_4] (0.010 g, 0.033 mmol), whereafter a CH_2Cl_2 solution (5 cm^3) containing a stoichiometric amount of *trans*-[FeH(NCCH=CHCN)$(dppe)_2$][BF_4] (**2a**, 0.031 g, 0.030 mmol) was added. The color changed immediately to dark blue and was kept with stirring for 2 h. It was then taken to dryness in vacuo. The solid residue was dissolved in CH_2Cl_2, the solution filtered and concentrated, and Et_2O added (with stirring) to give a dark blue precipitate of [{FeH$(dppe)_2$}$_2$(μ-NCCH=CHCN)][BF_4]$_2$ (**1a**, 0.033 g, 55% yield).

(3) Compound 1a. IR (KBr, cm^{-1}): 2165 (ν_{CN}). ^1H NMR: δ 7.42−6.81 (m, 80H, $(C_6H_5)_2PCH_2CH_2P(C_6H_5)_2$), 5.16 (s, 2H, C*H*=C*H*), 2.82 (m, 8H, 1/2$Ph_2PCH_2CH_2PPh_2$), 2.23 (m, 8H, 1/2$Ph_2PCH_2CH_2PPh_2$), −16.93 (qnt, J_{HP} = 48.0 Hz, 2H, Fe-*H*). $^{31}P\{^1H\}$ NMR: δ 82.2 (s, $Ph_2PCH_2CH_2PPh_2$). $^{31}C\{^1H\}$ NMR: δ 33.72 (qnt, J_{CP} = 12.1 Hz, $Ph_2PCH_2CH_2PPh_2$), 114.51 (s, NC*C*H=*C*HCN), 122.10 (s, N*C*CH=CH*C*N), 128.14 and 128.94 (s, C_m or C_o from dppe), 129.96 and 130.47 (s, C_p from dppe),132.71 and 133.38 (C_o or C_m from dppe), 134.58 (qnt, J_{CP} = 7.4 Hz, C_i from dppe), 135.40 (qnt, J_{CP} = 10.6 Hz, C_i from dppe). ^{31}C NMR: δ 33.72 (tqnt, J_{CH} = 135.2 Hz), 114.51 (d, J_{CH} = 179.5 Hz, 122.10 (s), 128.14 (d, J_{CH} = 164.4 Hz), 128.94 (d, J_{CH} = 161.3 Hz), 129.96 (d, J_{CH} = 160.7 Hz), 130.47 (d, J_{CH} = 162.5 Hz), 132.71 (d, J_{CH} = 160.6 Hz), 133.38 (d, J_{CH} = 161.3 Hz), 134.58 (m), 135.40 (m). Anal. Calcd for $C_{108}H_{100}B_2F_8N_2P_8Fe_2$: C, 65.8; H, 5.1; N, 1.4. Found: C, 65.6; H, 5.4; N, 1.4%. FAB mass: *m*/*z* 932 (M − FeH$(dppe)_2)^+$. UV/vis [λ_{max}/nm (ϵ/($M^{-1}\cdot cm^{-1}$))]: 615 (14 376) and 265 (43 558).

(4) Compound 1b. IR (KBr, cm^{-1}): 2184 (ν_{CN}). ^1H NMR: δ 7.49 (m, 16H, H_o from dppe), 7.37 (t, J_{HH} = 7.1 Hz, 8H, H_p from dppe), 7.29 (t, J_{HH} = 7.0 Hz, 8H, H_p from dppe), 7.18 (t, J_{HH} = 7.4 Hz, 16H, H_m from dppe), 7.13 (t, J_{HH} = 7.5 Hz, 16H, H_m from dppe), 6.82 (m, 16H, H_o from dppe), 6.72 (s, 4H, C_6H_4), 2.70 (m,

(46) (a) Happe, R. P.; Roseboom, W.; Pierik, A. J.; Albracht, S. P. J. *Nature* **1997**, *385*, 126. (b) Volbeda, A.; Charon, M.-H.; Piras, C.; Hatchikian, E. C.; Frey, M.; Fontecilla-Camps, J. C. *Nature* **1995**, *373*, 580. (c) Pavlov, M.; Siegbahn P. E. M.; Blomberg M. R. A.; Crabtree, R. H. *J. Am. Chem. Soc*. **1998**, *120*, 548.

(47) (a) Fryzuk, M. D.; Johnson, S. A. *Coord. Chem. Rev*. **2000**, *200*−*202*, 379. (b) Sellmann D.; Sutter, J. *Acc. Chem. Res*. **1997**, *30*, 460. (c) Richards, R. L. *Coord. Chem. Rev*. **1996**, *154*, 83. (d) Hidai, M.; Mizobe, Y. *Chem. Rev*. **1995**, *95*, 1115. (e) Bazhenova, T. A.; Shilov, A. E. *Coord. Chem. Rev*. **1995**, *144*, 69. (f) Eady, R. R.; Leigh, G. J. *J. Chem. Soc., Dalton Trans*. **1994**, 2739.

(48) Martins, L. M. D. R. S.; Fraústo da Silva, J. J. R.; Pombeiro, A. J. L.; Henderson, R. A.; Evans, D. J.; Benetollo, F.; Bombieri, G.; Michelin, R. A. *Inorg. Chim. Acta* **1999**, *291*, 39.

(49) (a) Martins, L. M. D. R. S.; Duarte, M. T.; Galvão, A. M.; Resende, C.; Pombeiro, A. J. L.; Henderson, R. A.; Evans, D. J. *J. Chem. Soc., Dalton Trans*. **1998**, 3311. (b) Guedes da Silva, M. F. C.; Martins, L. M. D. R. S.; Fraústo da Silva, J. J. R.; Pombeiro, A. J. L. *Collect. Czech. Chem. Commun*. **2001**, *66*, 139.

(50) Baptista, M. B.; Lemos, M. A. N. D. A.; Fraústo da Silva, J. J. R.; Pombeiro, A. J. L. *J. Organomet. Chem*. **1992**, *424*, 49.

(51) Meidine, M. F.; Lemos, M. A. N. D. A.; Pombeiro, A. J. L.; Nixon, J. F.; Hitchcock, P. B. *J. Chem. Soc., Dalton Trans*. **1998**, 3319.

(52) Almeida, S. S. P.; Duarte, M. T.; Ribeiro, L. M. D.; Gormley, F.; Galvão, A. M.; Fraústo da Silva, J. J. R.; Pombeiro, A. J. L. *J. Organomet. Chem*. **1996**, *524*, 63.

(53) Giannoccaro, P.; Sacco, A. *Inorg. Synth.* **1977**, *17*, 69.

8H, 1/2$Ph_2PCH_2CH_2PPh_2$), 2.18 (m, 8H, 1/2$Ph_2PCH_2CH_2PPh_2$), −17.93 (qnt, J_{HP} = 48.0 Hz, 2H, Fe-*H*). $^{31}P\{^1H\}$ NMR: δ 83.3 (s, $Ph_2PCH_2CH_2PPh_2$). $^{31}C\{^1H\}$ NMR: δ 33.40 (qnt, J_{CP} = 11.8 Hz, $Ph_2PCH_2CH_2PPh_2$), 115.93 (s, C_i from dinitrile), 124.67 (s, NCC_6H_4CN), 128.65 (s, C_m or C_o from dppe), 129.42 (s, C_m or C_o from dppe), 130.59 and 130.86 (s, C_p from dppe), 132.78 (s, C_o and C_m from dinitrile), 133.19 and 133.80 (s, C_o or C_m from dppe), 134.49 (qnt, J_{CP} = 7.1 Hz, C_i from dppe), 135.59 (qnt, J_{CP} = 9.1 Hz, C_i from dppe). ^{31}C NMR: δ 33.40 (tqnt, J_{CH} = 129.0 Hz), 115.93 (s), 124.67 (s), 128.65 (d, J_{CH} = 160.0 Hz), 129.42 (d, J_{CH} = 158.7 Hz), 130.59 (d, J_{CH} = 160.2 Hz), 130.86 (d, J_{CH} = 161.9 Hz), 132.78 (d, J_{CH} = 169.3 Hz), 133.19 (d, J_{CH} = 165.6 Hz), 133.80 (d, J_{CH} = 162.5 Hz), 134.49 (m), 135.59 (m). Anal. Calcd for $C_{112}H_{102}B_2F_8N_2P_8Fe_2$: C, 66.9; H, 5.1, N, 1.4. Found: C, 67.0; H, 5.0; N, 1.4%. FAB mass: *m*/*z* 1923 $(M + BF_4)^+$, 982 $(M - FeH(dppe)_2)^+$. UV/vis [λ_{max}/nm (ϵ/(M^{-1}·cm^{-1})]: 545 (12 282) and 265 (42 603).

(5) Compound 1c. IR (KBr, cm^{-1}): 2229 (ν_{CN}). ^1H NMR: δ 7.35−6.75 (m, 80H, $(C_6H_5)_2PCH_2CH_2P(C_6H_5)_2$), 2.84 (m, 8H, 1/2$Ph_2PCH_2CH_2PPh_2$), 2.12 (m, 8H, 1/2$Ph_2PCH_2CH_2PPh_2$), 2.12 (s, 4H, CH_2CH_2), −20.45 (qnt, J_{HP} = 44.6 Hz, 2H, Fe-*H*). $^{31}P\{^1H\}$ NMR: δ 81.6 (s, $Ph_2PCH_2CH_2PPh_2$). $^{31}C\{^1H\}$ NMR: δ 16.71 (s, $NCCH_2CH_2CN$), 33.85 (qnt, J_{CP} = 12.4 Hz, $Ph_2PCH_2CH_2PPh_2$), 125.88 (s, $NCCH_2CH_2CN$), 128.01 and 128.80 (s, C_m or C_o from dppe), 129.82 and 130.31 (s, C_p from dppe),132.74 and 133.47 (C_o or C_m from dppe), 135.78 (qnt, J_{CP} = 6.9 Hz, C_i from dppe), 136.13 (qnt, J_{CP} = 10.1 Hz, C_i from dppe). ^{31}C NMR: δ 16.71 (t, J_{CH} = 141.7 Hz), 33.85 (tqnt, J_{CH} = 134.0 Hz), 125.88 (s), 128.01 (d, J_{CH} = 163.7 Hz), 128.80 (d, J_{CH} = 160.5 Hz), 129.82 (d, J_{CH} = 161.3 Hz), 130.31 (d, J_{CH} = 161.3 Hz), 132.74 (d, J_{CH} = 160.6 Hz), 133.47 (d, J_{CH} = 160.0 Hz), 135.78 (m), 136.13 (m). Anal. Calcd for $C_{108}H_{102}B_2F_8N_2P_8Fe_2$: C, 64.0; H, 5.1; N, 1.4. Found: C, 64.0; H, 5.1; N, 1.4%. FAB mass: *m*/*z* 934 $(M - FeH(dppe)_2)^+$. UV/vis [λ_{max}/nm (ϵ/(M^{-1}·cm^{-1}))]: 440 (1 199) and 260 (33 392).

(b) Mononuclear Complexes *trans*-[FeH(LL)(dppe)$_2$][BF_4] (LL = NCCH═CHCN (2a), NCC_6H_4CN (2b), $NCCH_2CH_2CN$ (2c)). A procedure identical to that described above for the synthesis of the dinuclear complexes from *trans*-[FeHCl(dppe)$_2$] was applied, but by using a 5- to 10-fold molar excess of the appropriate dinitrile (LL), i.e. 0.172 g (2.20 mmol, for **2a**), 0.141 g (1.10 mmol, for **2b**), or 0.176 g (2.20 mmol, for **2c**). The products were also isolated similarly as above, as a violet (**2a**, 0.16 g, 71% yield), red (**2b**, 0.19 g, 78% yield), or yellow (**2c**, 0.16 g, 69% yield) solid.

(1) Compound 2a. IR (KBr, cm^{-1}): 2175 (ν_{CN}). ^1H NMR: δ 7.49−6.66 (m, 40H, $(C_6H_5)_2PCH_2CH_2P(C_6H_5)_2$), 5.81 (d, J_{HH} = 15.0 Hz, 1H, −NCCH═C*H*NC), 4.98 (d, J_{HH} = 15.3 Hz, 1H, −NCC*H*═CHNC), 2.64 (m, 4H, 1/2$Ph_2PCH_2CH_2PPh_2$), 2.11 (m, 4H, 1/2$Ph_2PCH_2CH_2PPh_2$), −16.07 (qnt, J_{HP} = 47.6 Hz, 1H, Fe-*H*). $^{31}P\{^1H\}$ NMR: δ 82.7 (s, $Ph_2PCH_2CH_2PPh_2$). $^{31}C\{^1H\}$ NMR: δ 32.68 (qnt, J_{CP} = 12.2 Hz, $Ph_2PCH_2CH_2PPh_2$), 114.81 (s, −NC*C*H═CHCN), 116.05 (s, −NCCH═CH*C*N), 118.38 (s, −NCCH═*C*HCN), 119.56 (s, −N*C*CH═CHCN), 128.28 and 129.04 (s, C_m or C_o from dppe), 130.42 and 130.64 (s, C_p from dppe),132.56 and 133.40 (C_o or C_m from dppe), 133.28 (qnt, J_{CP} = 7.7 Hz, C_i from dppe), 134.42 (qnt, J_{CP} = 10.7 Hz, C_i from dppe). ^{31}C NMR: δ 32.68 (tqnt, J_{CH} = 134.0 Hz), 114.81 (d, J_{CH} = 182.4 Hz), 116.05 (s), 118.38 (d, J_{CH} = 180.5 Hz), 119.56 (s), 128.28 (d, J_{CH} = 161.9 Hz), 129.04 (d, J_{CH} = 161.9 Hz), 130.42 (d, J_{CH} = 163.1 Hz), 130.64 (d, J_{CH} = 168.7 Hz), 132.56 (d, J_{CH} = 149.5 Hz), 133.40 (d, J_{CH} = 160.0 Hz), 133.28 (m), 134.42 (m). Anal. Calcd for $C_{56}H_{51}BF_4N_2P_4Fe$: C, 65.0; H, 5.0; N, 2.7;.Found: C, 64.7; H, 4.9; N, 2.6%. FAB mass: *m*/*z* 932 $(M)^+$. UV/vis [λ_{max}/nm (ϵ/(M^{-1}·cm^{-1}))]: 550 (11 778) and 270 (47 861).

(2) Compound 2b. IR (KBr, cm^{-1}): 2182 (ν_{CN}). ^1H NMR: δ 7.64 (d, J_{HH} = 8.4 Hz, 2H, H_m from dinitrile), 7.50 (m, 8H, H_o from dppe), 7.28 (m, 4H, H_p from dppe), 7.26 (m, 4H, H_p from dppe), 7.16 (t, J_{HH} = 7.4 Hz, 8H, H_m from dppe), 7.06 (t, J_{HH} = 7.8 Hz, 8H, H_m from dppe), 6.89 (d, J_{HH} = 8.7 Hz, 2H, H_o from dinitrile), 6.80 (m, 8H, H_o from dppe), 2.80 (m, 4H, 1/2$Ph_2PCH_2CH_2PPh_2$), 2.21 (m, 4H, 1/2$Ph_2PCH_2CH_2PPh_2$), −18.15 (qnt, J_{HP} = 47.2 Hz, 1H, Fe-*H*). $^{31}P\{^1H\}$ NMR: δ 81.6 (s, $Ph_2PCH_2CH_2PPh_2$). $^{31}C\{^1H\}$ NMR: δ 32.62 (qnt, J_{CP} = 12.1 Hz, $Ph_2PCH_2CH_2PPh_2$), 115.47 (s, C_i from dinitrile), 116.96 (s, C_p from dinitrile), 117.71 (s, $-NCC_6H_4CN$), 123.71 (s, $-NCC_6H_4CN$), 128.21 and 128.98 (s, C_m or C_o from dppe), 130.28 and 130.42 (s, C_p from dppe), 132.42 (s, C_m or C_o from dinitrile), 132.61 (C_o or C_m from dppe), 132.97 (s, C_o or C_m from dinitrile), 133.33 (s, C_o or C_m from dppe), 133.69 (qnt, J_{CP} = 7.2 Hz, C_i from dppe), 134.85 (qnt, J_{CP} = 10.6 Hz, C_i from dppe). ^{31}C NMR: δ 32.62 (tqnt, J_{CH} = 134.3 Hz), 115.47 (t, J_{CH} = 8.7 Hz, 116.96 (t, J_{CH} = 8.7 Hz), 117.71 (s), 123.71 (s), 128.21 (d, J_{CH} = 161.3 Hz), 128.98 (d, J_{CH} = 164.3 Hz), 130.28 (d, J_{CH} = 155.8 Hz), 130.42 (d, J_{CH} = 167.4 Hz), 132.42 (d, J_{CH} = 176.8 Hz), 132.61 (d, J_{CH} = 164.3 Hz), 132.97 (d, J_{CH} = 169.9 Hz), 133.33 (d, J_{CH} = 160.0 Hz), 133.69 (m), 134.85 (m). Anal. Calcd for $C_{60}H_{53}BF_4N_2P_4Fe$: C, 66.3; H, 4.9; N, 2.6. Found: C, 66.3; H, 5.2; N, 2.3%. FAB mass: *m*/*z* 982 $(M)^+$. UV/vis [λ_{max}/nm (ϵ/(M^{-1}·cm^{-1}))]: 490 (7 609) and 265 (34 855).

(3) Compound 2c. IR (KBr, cm^{-1}): 2230 (ν_{CN}). ^1H NMR: δ 7.47−6.76 (m, 40H, $(C_6H_5)_2PCH_2CH_2P(C_6H_5)_2$), 2.67 (m, 4H, 1/2$Ph_2PCH_2CH_2PPh_2$), 2.47 (t, J_{HH} = 6.0, 2H, $-NCCH_2CH_2NC$), 2.24 (t, J_{HH} = 6.4, 2H, $-NCCH_2CH_2NC$), 2.06 (m, 4H, 1/2$Ph_2PCH_2CH_2PPh_2$), −20.41 (qnt, J_{HP} = 46.9 Hz, 1H, Fe-*H*). $^{31}P\{^1H\}$ NMR: δ 81.6 (s, $Ph_2PCH_2CH_2PPh_2$). $^{31}C\{^1H\}$ NMR: δ 14.26 (s, $-NCCH_2CH_2CN$), 17.88 (s, $-NCCH_2CH_2CN$), 32.82 (qnt, J_{CP} = 11.9 Hz, $Ph_2PCH_2CH_2PPh_2$), 117.75 (s, $-NCCH_2CH_2CN$), 126.40 (s, $-NCCH_2CH_2CN$), 128.05 and 128.91 (s, C_m or C_o from dppe), 130.22 (s, C_p from dppe),132.63 and 133.38 (C_o or C_m from dppe), 134.44 (qnt, J_{CP} = 7.1 Hz, C_i from dppe), 135.59 (qnt, J_{CP} = 10.4 Hz, C_i from dppe). ^{31}C NMR: δ 14.26 (t, J_{CH} = 138.3 Hz), 17.88 (t, J_{CH} = 139.6 Hz), 32.82 (tqnt, J_{CH} = 134.0 Hz), 117.75 (s), 126.40 (s), 128.05 (d, J_{CH} = 162.5 Hz), 128.91 (d, J_{CH} = 161.9 Hz), 130.22 (d, J_{CH} = 156.1 Hz), 132.63 (d, J_{CH} = 160.0 Hz), 133.38 (d, J_{CH} = 160.0 Hz), 134.44 (m), 135.59 (m). Anal. Calcd for $C_{56}H_{53}BF_4N_2P_4Fe$: C, 63.8; H, 5.1; N, 2.6. Found: C, 64.0; H, 5.2; N, 2.4%. FAB mass: *m*/*z* 934 $(M)^+$. UV/vis [λ_{max}/nm (ϵ/(M^{-1}·cm^{-1}))]: 440 (964) and 260 (18 932).

Electrochemistry. The electrochemical experiments were performed on an EG&G PARC 273 potentiostat/galvanostat connected to a PC computer through a GPIB interface (National Instruments PC-2A). Cyclic voltammetry (CV) experiments were undertaken in a two-compartment three-electrode cell, at a platinum−disk (or vitreous carbon disk) working electrode probed by a Luggin capillary connected to a silver-wire pseudo-reference electrode; a platinum auxiliary electrode was employed. Controlled potential electrolyses (CPE) were carried out in a two-compartment three-electrode cell with platinum-gauze working and counter electrodes in compartments separated by a glass frit; a Luggin capillary, probing the working electrode, was connected to a silver wire pseudo-reference electrode. The electrochemical experiments were performed in a N_2 atmosphere at room temperature. The potentials were measured by CV in 0.2 mol dm^{-3} [NBu_4][BF_4]/CH_2Cl_2, and the values are quoted relative to the saturated calomel electrode (SCE) by using the *trans*-[FeHCl(dppe)$_2$]$^{0/+}$ redox couple ($E°$ = −0.143 V vs SCE in CH_2Cl_2) as the internal standard. The IUPAC recommended ferrocene/ferricinium redox couple was not used for

Scheme 1. Syntheses of the Dinitrile Complexes **1** and **2**

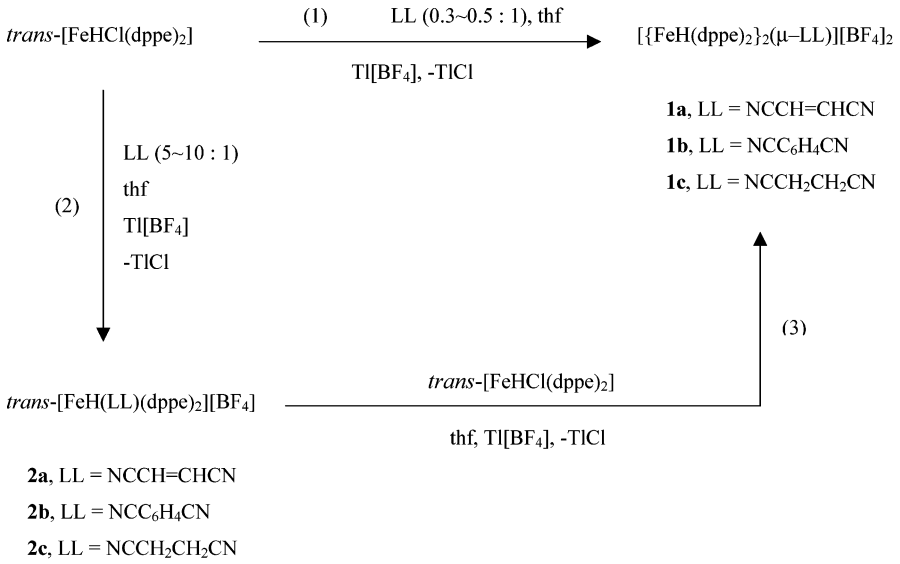

this purpose on account of the partial overlap of its wave ($E_{1/2}^{ox}$ = 0.525 V vs SCE in CH_2Cl_2) with the first ones of our complexes. The CPE experiments were monitored regularly by CV to ensure that no significant potential drift occurred along the electrolyses. The acid−base potentiometric titrations were carried out by using a standard solution of KOH in methanol. The results were corrected for background effects by performing also the titration of a blank solution of the electrolyte, which has been electrolyzed under conditions identical to those used for the corresponding complex solution. The corrected values are the following ones: $1H^+$ when the CPE was performed at the oxidation wave of the mononuclear complexes or at the first oxidation wave of the dinuclear complex **1a** and $2H^+$ when the CPE was carried out at the second oxidation wave of the latter compound.

The mechanism of the oxidation processes was investigated by digital simulation (program ESP[54]) of the cyclic voltammograms at different scan rates (in the 0.4−60 V s^{-1} range). The $E°$ and k_{het} values for the electron-transfer processes were chosen in order to allow a close correspondence between simulated and experimental cyclic voltammograms for the entire range of scan rates of the CV experiments.

Theoretical Studies. The full geometry optimization of the structures has been carried out in Cartesian coordinates using the *quasi*-Newton−Raphson gradient method and the restricted (for close-shell structures) or unrestricted (for open-shell structures) Hartree−Fock approximation with help of the GAMESS[55] and Gaussian 98[56] program packages. Symmetry operations were not applied for all structures. The standard basis set of Gauss functions 6-31G[57] was selected for all atoms. The single-point calculations of the several structures have been performed at the MP2 level of theory on the basis of the equilibrium Hartree−Fock geometries. The solvent effects were taken into account for the mononuclear complexes by using the polarizable continuum model[58] in the CPCM version[59] with CH_2Cl_2 and thf as solvents.

As it was previously shown,[60] the use for the calculations of the model structures with two monodentate PH_3 ligands instead of the chelate dppe ligand does not affect significantly the structural, electronic, and energetic properties of the complexes. Thus, the hypothetical dinuclear complexes $[\{FeH(PH_3)_4\}_2(\mu\text{-LL})]^{n+}$ (LL = NC−CH=CH−CN and NC−CH_2–CH_2–CN, n = 2, 3, 4) and the corresponding deprotonated species, as well as the mononuclear complexes $[Fe(NCCH_3)(PH_3)_4]^{2+}$ and $[FeF(NCCH_3)(PH_3)_4)]^+$ were chosen as model compounds for our calculations instead of the real complexes with two dppe ligands at each metal site. The choice of the basis set and of the model of the complex took into account a reasonable computational time required for geometry optimization.

Results and Discussion

Syntheses. Treatment at room temperature of a thf solution of *trans*-[FeHCl(dppe)$_2$], in the presence of Tl[BF_4] as the halide abstracting agent, with the appropriate dinitrile (LL) in a molar defficiency (LL:complex molar ratio not higher than 0.5:1), leads to the formation (Scheme 1 (eq 1)) of the corresponding dinuclear complexes with bridging dinitriles $[\{FeH(dppe)_2\}_2(\mu\text{-LL})][BF_4]_2$ (LL = NCCH=CHCN (**1a**), NCC_6H_4CN (**1b**), $NCCH_2CH_2CN$ (**1c**)), which were isolated as blue (**1a**), red (**1b**), or yellow (**1c**) solids in ca. 80−50% yields. If the reaction is performed in similar experimental conditions but using an excess of the dinitrile (5- to 10-fold

(54) Nervi, C. (nervi@lem.ch.unito.it). *Electrochemical Simulation Package* (ESP, version 2.4); Dipartimento di Chimica IFM: Torino, Italy, 1994/98.

(55) Schmidt, M. W.; Baldridge, K. K.; Boatz, J. A.; Elbert, S. T.; Gordon, M. S.; Jensen, J. H.; Koseki, S.; Matsunaga, N.; Nguyen, K. A.; Su, S. J.; Windus, T. L.; Dupuis, M.; Montgomery, J. A. *J. Comput. Chem.* **1993**, *14*, 1347.

(56) Frisch, M. J.; Trucks, G. W.; Schlegel, H. B.; Scuseria, G. E.; Robb, M. A.; Cheeseman, J. R.; Zakrzewski, V. G.; Montgomery, J. A., Jr.; Stratmann, R. E.; Burant, J. C.; Dapprich, S.; Millam, J. M.; Daniels, A. D.; Kudin, K. N.; Strain, M. C.; Farkas, O.; Tomasi, J.; Barone, V.; Cossi, M.; Cammi, R.; Mennucci, B.; Pomelli, C.; Adamo, C.; Clifford, S.; Ochterski, J.; Peterson, G. A.; Ayala, P. Y.; Cui, Q.; Morokuma, K.; Malick, D. K.; Rabuck, A. D.; Raghavachari, K.; Foresman, J. B.; Cioslowski, J.; Ortiz, J. V.; Baboul, A. G.; Stefanov, B. B.; Liu, G.; Liashenko, A.; Piskorz, P.; Komaromi, I.; Gomperts, R.; Martin, R. L.; Fox, D. J.; Keith, T.; Al-Laham, M. A.; Peng, C. Y.; Nanayakkara, A.; Challacombe, M.; Gill, P. M. W.; Johnson, B.; Chen, W.; Wong, M. W.; Andres, J. L.; Gonzalez, C.; Head-Gordon, M.; Replogle, E. S.; Pople, J. A. *Gaussian 98*, Revision A.9; Gaussian, Inc.: Pittsburgh, PA, 1998.

(57) Rassolov, V.; Pople, J. A.; Ratner, M.; Windus, T. L. *J. Chem. Phys.* **1998**, *109*, 1223, and references therein.

(58) Tomasi, J.; Persico, M. *Chem. Rev.* **1997**, *94*, 2027.

(59) Barone, V.; Cossi, M. *J. Phys. Chem.* **1998**, *102*, 1995.

(60) Zhang, L.; Guedes da Silva, M. F. C.; Kuznetsov, M. L.; Gamasa, M. P.; Gimeno, J.; Fraústo da Silva, J. J. R.; Pombeiro, A. J. L. *Organometallics* **2001**, *20*, 2782.

molar ratio), the corresponding mononuclear complexes *trans*-[FeH(LL)(dppe)$_2$][BF$_4$] (LL = NCCH=CHCN (**2a**), NCC$_6$H$_4$CN (**2b**), NCCH$_2$CH$_2$CN (**2c**)) are the obtained products [Scheme 1 (eq 2)], isolated as violet (**2a**), red (**2b**), or yellow (**1c**) solids in ca. 78−70% yields. Further treatment of the mononuclear complexes **2** with the starting *trans*-[FeHCl(dppe)$_2$] complex, also in thf and in the presence of Tl[BF$_4$], yields the corresponding dinuclear complexes **1** [Scheme 1 (3)] formed upon coordination of the hanging nitrile function of the monodentate dinitrile ligand of **2** to the added iron(II) center. However, this alternative route (2−3) for the dinuclear complexes **1** is less convenient than the above route (1) which is more direct, faster, and presents higher yields.

The complexes have been characterized by IR, UV/vis, and multinuclear magnetic resonance spectroscopies, elemental analysis, FAB$^+$-MS spectrometry, and electrochemical methods. In their IR spectra, ν(N≡C) appears as bands at ca. 2165−2175 (with a strong intensity, **1a** or **2a**), ca. 2183 (medium, **1b** or **2b**), or ca. 2230 cm^{-1} (weak, **1c** or **2c**), corresponding to coordination shifts $\Delta\nu = \nu(\text{N}{\equiv}\text{C})_{\text{ligand}} - \nu(\text{N}{\equiv}\text{C})_{\text{free nitrile}}$ of ca. −65 to −75 (LL = NCCH=CHNC), ca. −48 (LL = NCC$_6$H$_4$CN), or ca. −25 (LL = NCCH$_2$-CH$_2$CN) cm^{-1}. The ν(N≡C) shift to lower wavenumbers upon coordination is indicative of a significant π-electron effect in the decreasing order of NCCH=CHNC > NCC$_6$H$_4$-CN > NCCH$_2$CH$_2$CN. The ν(N≡C) values fall in the range known[61] for related mononitrile complexes (2205−2250 cm^{-1}) and are higher than those observed for the isocyanide complexes *trans*-[FeH(CNR)(dppe)$_2$]$^+$ (R = H,[8] alkyl,[50] or aryl[50]) or the related isocyanotriphenylborate complex *trans*-[FeH(CNBPh$_3$)(dppe)$_2$],[8] in accord with the expected[62] stronger π-electron acceptor ability of the isocyanide compared with the nitrile ligands.

The trans geometry of the complexes is assigned on the basis of the singlet resonance observed in their ^{31}P{^{1}H} NMR spectra, whereas the presence of the hydride ligand is accounted for by the high-field (δ ca. −16 to −20) quintet ($^2J_{\text{HP}}$ ca. 45−48 Hz) resonance exhibited by the ^{1}H NMR spectra. In the ^{13}C{^{1}H} NMR spectra, the N*C* resonances of the ligated dinitriles in the dinuclear complexes **1** appear as one singlet at δ ca. 122−126, while in the mononuclear compounds **2** two singlets are observed (e.g at δ 119.56 and 116.05 for **2a**) on account of the nonequivalence of the two NC groups of the η^1-dinitrile ligands. All the other resonances of the dinitrile and dppe ligands have also been assigned in both the ^{1}H and the ^{13}C NMR spectra, including those of the ipso-, ortho-, meta-, and para-atoms of the phenyl rings.

Electrochemical Studies. The electrochemical behavior of the mono- and dinuclear complexes in 0.2 mol dm^{-3} [NBu$_4$][BF$_4$]/CH$_2$Cl$_2$ was studied by cyclic voltammetry (CV) and controlled potential electrolysis (CPE), at a Pt-disk (or vitreous C disk) or a Pt-gauze electrode, respectively. Relevant data are indicated in Table 1.

Table 1. Cyclic Voltammetric Data[a] for [{FeH(dppe)$_2$}$_2$(μ-LL)][BF$_4$]$_2$ (**1**) and *trans*-[FeH(LL)(dppe)$_2$][BF$_4$] (**2**)

complex	$^{\text{I}}E_{1/2}^{\text{ox}}$/V	$^{\text{II}}E_{\text{p/2}}^{\text{ox}}$/V	$E_{1/2}^{\text{red}}$ ($E_{\text{p/2}}^{\text{red}}$)/V
1a	0.68	0.86	0.98
1b	0.69		1.30
1c	0.64		
2a	0.72		(1.07)
2b	0.70		1.29
2c	0.63		-

[a] Potentials (half-wave potential $E_{1/2}$ for the reversible processes or half-height peak potential $E_{\text{p/2}}$ for the irreversible ones, in V ± 0.02 vs SCE) measured in 0.2 mol dm^{-3} [NBu$_4$][BF$_4$]/CH$_2$Cl$_2$ at a scan rate of 0.4 V s^{-1} and at a Pt-disk (d = 0.5 mm) electrode.

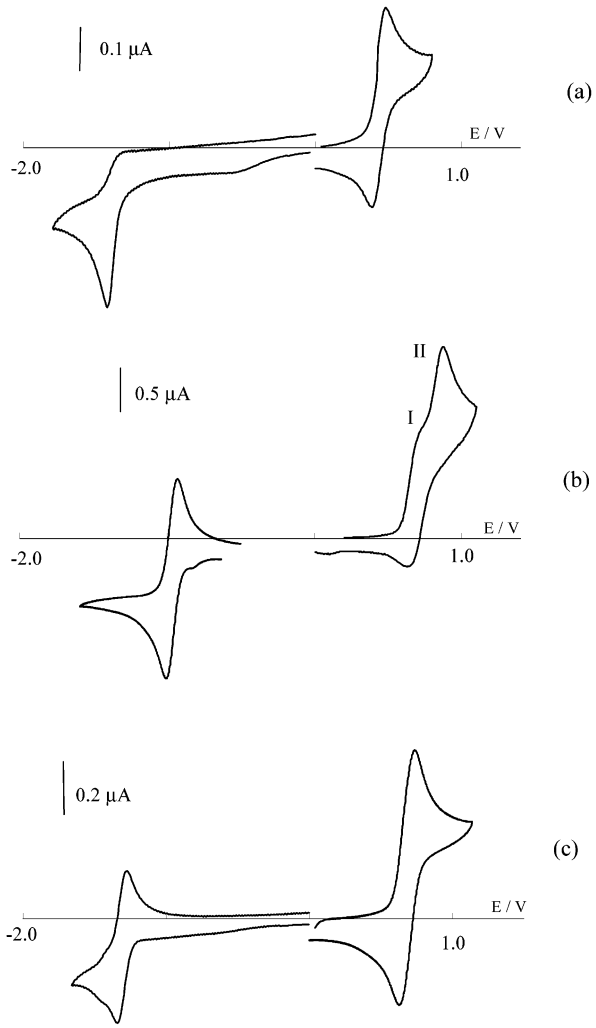

Figure 1. Cyclic voltammograms of complexes **2a** (1.06 mM) (a), **1a** (1.35 mM) (b), and **1b** (0.51 mM) (c), in CH$_2$Cl$_2$ with 0.2 M [NBu$_4$][BF$_4$] at a platinum disk (d = 0.5 mm) working electrode. Potentials are given in volts vs SCE. Scan rate: 0.2 V s^{-1}.

Mononuclear Complexes 2. The cyclic voltammograms of complexes **2** display one single-electron reversible oxidation wave (Figure 1a for complex 2a) at a potential ($E_{1/2}^{\text{ox}}$) ranging from 0.63 to 0.72 V vs SCE, attributed to the reversible Fe$^{\text{II}}$ → Fe$^{\text{III}}$ oxidation, and one single-electron partially reversible ($E_{1/2}^{\text{red}}$ = −1.29 V, **2b**) or irreversible ($E_{\text{p/2}}^{\text{red}}$ = −1,07 V, **2a**) reduction wave which is believed to be ligand centered (the cyclic voltammograms, run at similar experimental conditions, of free terephthalonitrile and fu-

(61) Giannoccaro, P.; Rossi, M.; Sacco, A., *Coord. Chem. Rev.* **1972**, *8*, 77.
(62) Pombeiro, A. J. L. *New J. Chem.* **1997**, *21*, 649.

maronitrile present reduction waves at $E_{1/2}^{red} = -1.59$ V and $E_{p/2}^{red} = -1.11$, respectively, thus revealing a significant anodic shift of the ligand centered reduction processes upon coordination). However, the anodic CPE at the oxidation wave of any of the complexes consumes 2F/mol and leads to proton extrusion (overall $-2e^-/-H^+$ process). The liberated proton was detected by its broad cathodic wave at E_p^{red} ca. -0.3 V (which undergoes an extensive cathodic shift on replacement of Pt by vitreous carbon as the working electrode material) and by potentiometric titration of the electrolyzed solution. Hence, in the extended time scale of the CPE, anodically induced proton loss occurs upon Fe−H bond cleavage, conceivably according to the process shown by reactions 1 ($E_2^{ox} \leq E_1^{ox}$), in which *Fe* = *trans*-{Fe(LL)-(dppe)$_2$}, as known for the related *trans*-[FeH(L)(dppe)$_2$]^n (L = CNR, $n = 1$;[9] L = CN, $n = 0$[8]) complexes. The heterolytic M−H bond cleavage results from the increase of the acidity character upon metal oxidation, as corroborated by theoretical studies (see below) and is also documented in other hydride complexes.[2−7]

$$[Fe^{II}-H]^+ \overset{(E_1^{ox})}{\underset{-e}{\rightleftharpoons}} [Fe^{III}-H]^{2+} \xrightarrow{-H^+} [Fe^{I}]+ \overset{(E_2^{ox})}{\underset{-e}{\rightleftharpoons}} [Fe^{II}]^{2+} \quad (1)$$

Dinuclear Complexes 1. Complexes **1** exhibit, by CV, at a scan rate of 0.2 V s^{-1}, one (partially) reversible anodic wave at $E_{1/2}^{ox} = 0.64-0.69$ V vs SCE (wave I) which, for compound **1a** (Figure 1b), is followed, at a slightly higher potential ($^{II}E_{p/2} = 0.86$ V), by a second one (wave II) with an irreversible character.

The observation of two anodic waves (assigned to the two sequential $Fe^{II} \rightarrow Fe^{III}$ oxidations) only for compound **1a** can be attributed to an interaction between the two iron centers propagated throughout the orbitals of the conjugated bridging N≡C−C═C−C≡N framework. In contrast, for compounds **1b** (Figure 1c) and **1c** only one anodic wave is detected for both $Fe^{II} \rightarrow Fe^{III}$ oxidations, showing that incorporating a phenyl ring or a saturated carbon group between the two cyano units hampers such an interaction to an extent that it is not detected. Other features of the anodic behavior are described below.

Reversible ligand centered single-electron cathodic waves are also detected at $E_{1/2}^{red} = -0.98$ (**1a**) or -1.30 (**1b**) V, in the latter case with the peak current intensity quite lower than (less than half) that of the oxidation wave, corroborating the involvement of both Fe^{II} centers in the oxidation process.

Estimate of Electrochemical Ligand Parameters. The measured oxidation potentials ($^{I}E_{1/2}^{ox}$) of the complexes **1** (also $E_{p/2}^{ox}$ for **1a**) and **2**, viewed as closed shell octahedral-type complexes [M_SL] with the ligand L ligating the 16-electron {M_S} = *trans*-{FeH(dppe)$_2$}$^+$ site, allows one to estimate the electrochemical P_L ligand constant (a measure of the net π-electron acceptor minus σ-donor character of a ligand), by applying the linear relationship (2) between $E_{1/2}^{ox}$ and P_L (for ligand L)[63] to our complexes and considering the known[63] values of the electron richness ($E_S = 1.04$ V) and polarizability ($\beta = 1.0$) for their iron(II) binding site.

$$E_{1/2}^{ox}[M_SL] = E_S + \beta P_L \quad (2)$$

Table 2. Estimated P_L and E_L Ligand Parameters

ligand	P_L/V	E_L[a]/V
NCCH═CHCN	0.32	0.46
NCC_6H_4CN	0.34	0.44
$NCCH_2CH_2CN$	0.41	0.39
NCCH═CHCN{$Fe^{II}H(dppe)_2$}$^+$ (**2a**)	0.36	0.43
NCCH═CHCN{$Fe^{III}H(dppe)_2$}$^{2+}$ (**2a**$^+$)	0.18	0.58
NCC_6H_4CN{$Fe^{II}H(dppe)_2$}$^+$ (**2b**)	0.35	0.44
NCC_6H_4CN{$Fe^{III}H(dppe)_2$}$^{2+}$ (**2b**$^+$)	0.35	0.44
$NCCH_2CH_2CN${$Fe^{II}H(dppe)_2$}$^+$ (**2c**)	0.40	0.39
$NCCH_2CH_2CN${$Fe^{III}H(dppe)_2$}$^{2+}$ (**2c**$^+$)	0.40	0.39

[a] In V vs NHE.

The thus obtained P_L values (Table 2) show that (i) the net electron acceptor/donor ability of the dinitrile ligands follow the order NCCH═CHCN ($P_L = -0.32$ V) ≥ NCC_6H_4CN ($P_L = -0.34$ V) > $NCCH_2CH_2CN$ ($P_L = -0.41$ V), (ii) neither the coordination of one of the cyano groups of NCC_6H_4CN or $NCCH_2CH_2CN$ to {FeH(dppe)$_2$}$^+$ nor the oxidation of this metal center affects significantly the electron acceptor/donor character of the other NC group, since no appreciable variation of P_L occurs [-0.35 or -0.40 V for the ligands NCC_6H_4CN{FeH(dppe)$_2$}^{n} ($n = +1$ (**2b**) and $+2$ (**2b**$^+$)) or $NCCH_2CH_2CN${FeH(dppe)$_2$}^{n} ($n = +1$ (**2c**) and $+2$ (**2c**$^+$)), respectively], and (iii) for NCCH═CHCN its coordination to {FeH(dppe)$_2$}$^+$ appears to lead to a slight decrease of the π-electron acceptor/σ-donor character of the other cyano group (P_L slightly decreases from -0.32 for NCCH═CHCN to -0.36 V for NCCH═CHCN{FeH-(dppe)$_2$}$^+$ (**2a**)), whereas oxidation of the iron(II) center results in a substantial increase of that character (P_L increases to -0.18 V for NCCH═CHCN{FeH(dppe)$_2$}$^{2+}$ (**2a**$^+$)). These observations indicate that NCCH═CHCN has a net π-electron acceptor/σ-donor ability identical to (or even marginally stronger than) that of the aromatic NCC_6H_4CN nitrile and is the only one that allows an electronic interaction to be noticed between the two metal centers. In comparison with related ligands,[62] all the above dinitriles (P_L in the range from -0.41 to -0.18 V) behave as more effective net electron acceptor/donor ligands than acetonitrile ($P_L = -0.58$ V),[63] isocyanotriphenylborate $CNBPh_3^-$ ($P_L = -0.51$ V)[8] or cyanide ($P_L = -1.0$ V).[63]

The values of the E_L ligand parameter (an additive parameter based on an empirical redox potential parametrization method[64] distinct from the above, but that reflects, like P_L, although in a different scale, the net electron acceptor/donor character of a ligand) were also estimated (Table 2) for the above ligands, by using the empirical relationship $P_L = 1.17E_L - 0.86$ [64] between P_L and that parameter. The same conclusions on the relative ligand electron acceptor/donor abilities as the above based on P_L can be drawn from comparisons of the E_L values.

(63) Chatt, J.; Kan, C. T.; Leigh, G. J.; Pickett, C. J.; Stanley, D. R. *J. Chem Soc., Dalton Trans.* **1980**, 2032.

(64) Lever, A. B. P. *Inorg. Chem.* **1990**, *29*, 1271.

(65) Richardson, D. E.; Taube, H. *Inorg. Chem.* **1981**, *20*, 1278, and references therein.

Scheme 2. Proposed Mechanism for the Anodic Processes of the Complex $[\{FeH(dppe)_2\}_2(\mu\text{-NCCH=CHCN})][BF_4]_2$, **1a**[a]

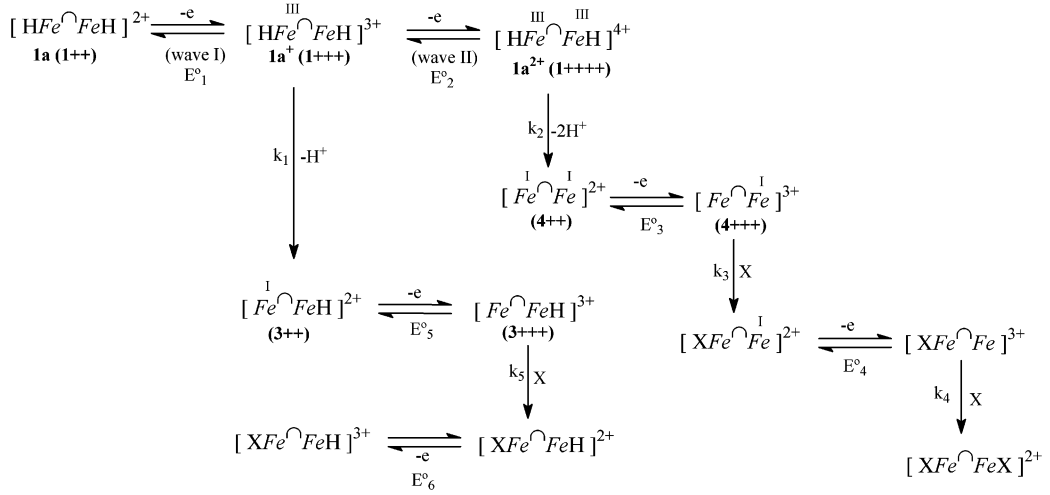

[a] The numbers in parentheses (**1**++, **1**+++, etc.) are those of the model complexes of the theoretical studies. Only the metal oxidation states different from II are indicated. X indicates an (anionic) nucleophile (see text)

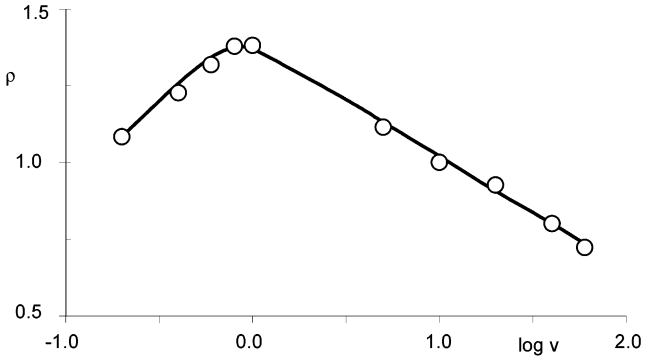

Figure 2. Experimental (symbols) and theoretical (line) variation of $\rho = i_p^{II}/i_p^{I}$ (see text) as a function of log scan rate. The solid line corresponds to the working curve for the mechanism described in Scheme 2.

Mechanistic Study of the Oxidation Process of 1a. The cyclic voltammetric behavior of dinuclear complex **1a**, denoted in a simplified way by $[HFe\frown FeH]^{2+}$, was studied in detail, showing a marked dependence on the scan rate. Hence, at sufficiently high scan rates there is no time for the occurrence, at a considerable extent, of any chemical reaction and each oxidation (I and II) tends to a single-electron reversible oxidation. This limiting behavior corresponds to the reversible $Fe^{II} \rightarrow Fe^{III}$ oxidation of each metal center to form $[HFe\frown FeH]^{3+}$ (wave I) and $[HFe\frown FeH]^{4+}$ (wave II, Scheme 2). However, upon lowering the scan rate, (i) the anodic current function $i_p^{ox}v^{-1/2}C^{-1}$ (i_p^{ox} = anodic peak current, v = scan rate, and C = concentration) increases for both waves, mainly for wave II (by a factor of ca. 3 from v = 60 V s^{-1} to 0.4 V s^{-1}), until, for sufficiently low scan rates, that of wave I increases faster than that of wave II, as shown by the ratio of the peak current intensities of these waves ($\rho = {}^{II}i_p^{ox}/{}^{I}i_p^{ox}$), which (Figure 2, symbols) increases with the decrease of the scan rate until reaching a maximum and then lowering for the lowest scan rates. Moreover, the reversible character of the waves, mainly wave II, also decreases with lowering of the scan rate.

Hence, the increase of the time of the experiment (decrease of scan rate) allows the occurrence of chemical reactions of the oxidized species, at both oxidation waves, with formation of products that are further oxidized (an increase of the number of electrons involved), and the relative extent of the two wave processes is also dependent on that time. The cyclic voltammetric behavior does not appear to depend on the complex concentration, thus ruling out second-order processes on that concentration, in contrast to what was observed[2c,e,10] in other metal−hydride systems. However, first-order ET-induced M−H bond cleavage processes are also known in other cases.[2a,3b,c,4,8,9]

CPE at the onset of the anodic wave I led to the consumption of 2F/mol with liberation of $1H^+$/molecule as indicated (see above) by CV experiments and acid−base titration of the electrolized solution and expected on the basis of theoretical studies (see below). The final obtained product presents a reversible anodic wave at $E_{1/2}^{ox}$ = 0.77 V, as shown by the cyclic voltammogram run after the electrolysis. Exhaustive anodic CPE at the oxidation wave II of compounds **1a** (or at the unique oxidation wave for any of the other dinuclear complexes) led to the overall (waves I and II) consumption of 4F/mol, with liberation of $2H^+$/molecule as also indicated by CV and measured by acid−base titration of the electrolyzed solution. Hence, an overall $-2e^-/-H^+$ process per each iron site occurs for any of the dinuclear complexes, as observed (see above) for the mononuclear compounds **2**.

Anodically induced proton loss upon heterolytic $Fe^{III}-H$ bond cleavage is not the only expected chemical reaction. In fact, a concomitant $Fe^{III} \rightarrow Fe^{I}$ reduction (the two electrons of that bond are transferred to the metal) occurs and the generated Fe^{I} center is expected (see theoretical studies) to be oxidized at a potential not significantly higher than that of the parent $Fe^{II} \rightarrow Fe^{III}$ oxidation, to form an unsaturated Fe^{II} tricationic species (Scheme 2). This should readily undergo nucleophilic attack, e.g. by the electrolyte anion, BF_4^-, as we have observed[9] for the related isocyanide complexes *trans*-$[FeH(CNR)(dppe)_2]^+$ (R = alkyl or aryl) which follow a complex oxidation process that can be described by an ECEC-type reaction mechanism with the

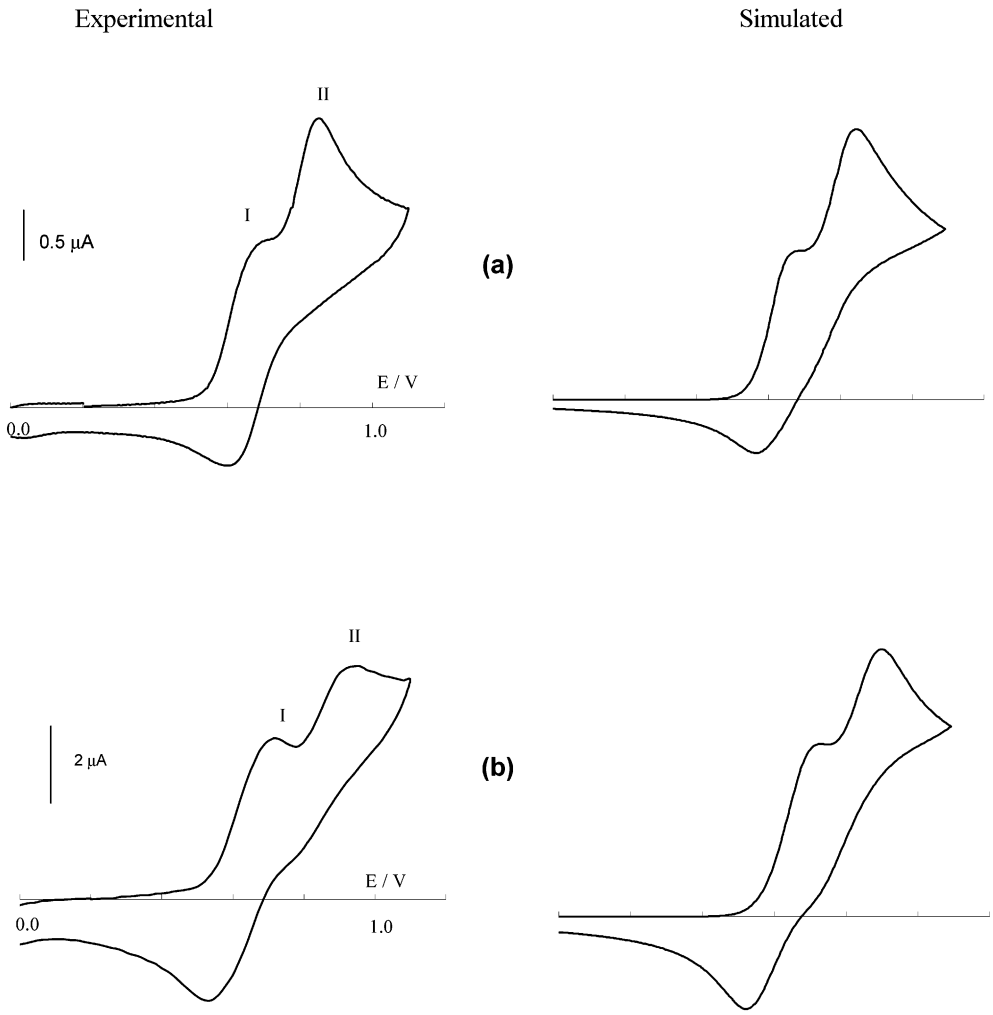

Figure 3. Experimental (left) and simulated (right) cyclic voltammograms of complex **1a** (1.35 mM, in CH_2Cl_2, with 0.2 M [NBu_4][BF_4]) at a platinum disk (d = 0.5 mm) working electrode. Potentials are given in volts vs SCE. Scan rate: 0.4 (a) and 20 V s^{-1} (b).

first chemical (C) step consisting of H^+ extrusion from the oxidized original complex and the second one involving attack of BF_4^- to the thus formed unstable iron(I) species. The obtained metal fluorinated product $[FeF(CNR)(dppe)_2]^+$ could be reversibly oxidized at a slightly higher potential. In the present study, the nature of the final products could not be established since attempts for their isolation and full characterization have failed. Hence, the nucleophilic reagent is denoted by X in Scheme 2, but theoretical calculations (see below) suggest that BF_4^- is a rather plausible one.

Cyclic voltammetric simulations[54] were used to validate quantitatively the processes given in Scheme 2 (variations thereof or other reaction schemes could not be simulated successfully) and to obtain kinetic data for the deprotonation and the nucleophilic attack reactions. A good fit was obtained for the following optimized values of $E°$ and chemical rate constants: $E°_1$ = 0.61 V, $E°_2$ = 0.80 V, $E°_3 = E°_5$ = 0.58 V, $E°_4$ = 0.67 V, and $E°_6$ = 0.78 V; k_1 = 4.5 s^{-1}, k_2 = 50 s^{-1}, k_3[X] = 0.25 s^{-1}, and k_4[X] = k_5[X] = 0.01 s^{-1} (i.e. k_3 = 1.25 M^{-1} s^{-1} and $k_4 = k_5$ = 0.05 M^{-1} s^{-1}, assuming that X = BF_4^-). The agreement between the experimental and the simulated data is illustrated in Figure 3 for the scan rates of 0.4 and 20 V s^{-1} and is also shown by the plot (Figure 2) of the experimental (symbols) and simulated (line) current ratio $\rho = {}^{II}i_p^{ox}/{}^{I}i_p^{ox}$ as a function of log scan rate.

By using the $E°$ values obtained by simulation, the comproportionation constant $K_C = \exp|n_1E°_1 - n_2E°_2|/25.69$ (at 298 K, with $E°$ in millivolts),[65] i.e. the equilibrium constant of reaction 3 ($n_1 = n_2 = 1$; $|E°_1 - E°_2|$ = 190 mV), was calculated. It indicates the stabilization of the mixed-valence Fe^{II}–Fe^{III} state in **1a** and reflects the interaction between the metals. The obtained value of $K_C = 1.6 \times 10^3$ is indicative of a class II mixed valence system (delocalization takes place but the two types of site are distinguishable).[66] It is much lower than that (1.6×10^{12}, in CH_2Cl_2) for $[\{Fe(Cp^*)(dppe)\}_2(\mu\text{-}C{\equiv}CC{\equiv}C)]$[32c] ($Cp^* = \eta^5\text{-}C_5Me_5$), comparable to those of $[\{Cr(CO)_3\}_2(biphenyl)]$[67] ($2.5 \times 10^3$, in CH_2Cl_2), $[\{Cr(CO)_2(PPh_3)\}_2(biphenyl)]$[67] ($2.6 \times 10^4$, in CH_2Cl_2), or $[\{Fe(Cp^*)(dppe)\}_2(\mu\text{-}C{\equiv}C{-}C_6H_4{-}C{\equiv}C)]$[32c] ($2.6 \times 10^4$) and higher than those for several weakly coupled class II dipyridyl-bridge bis(pentaammineruthenium) binuclear complexes[68] (K_C ranging from 4 to 890, in water).

(66) Robin, M. B.; Day, P. *Adv. Inorg. Chem. Radiochem*. **1967**, *10*, 247.
(67) Van Order, N., Jr.; Geiger, W. E.; Bitterwolf, T. E.; Rheingold, A. L. *J. Am. Chem. Soc.* **1987**, *109*, 5680.
(68) Creutz, C. *Prog. Inorg. Chem.* **1983**, *30*, 1, and references therein.

$$[\mathrm{HFe}^{\frown}\mathrm{FeH}]^{2+} + [\mathrm{HFe^{III}}^{\frown}\mathrm{Fe^{III}H}]^{4+} \overset{K_C}{\rightleftharpoons} [\mathrm{HFe^{III}}^{\frown}\mathrm{FeH}]^{3+} \quad (3)$$

Theoretical Studies. $[\{FeH(PH_3)_4\}_2(\mu\text{-}N{\equiv}C{-}CH{=}CH{-}C{\equiv}N)]^{2+}$ (**1**++) and $[\{FeH(PH_3)_4\}_2(\mu\text{-}N{\equiv}C{-}CH_2{-}CH_2{-}C{\equiv}N)]^{2+}$ (**2**++), as models for complexes **1a** and **1c**, respectively, as well as their oxidized forms and products of deprotonation have been investigated by theoretical methods. For the starting ones the geometry optimization of both isomeric forms of the bridging ligand (i.e. *E* or *Z* for N≡CCH═CHC≡N and anti or syn for $N{\equiv}CCH_2{-}CH_2C{\equiv}N$) has been performed. Each model complex is referenced according to the bridge isomer followed by a number and the charge.

Equilibrium Structure, MO Composition, Oxidation Potential, and Interaction between the Metals. For all equilibrium structures, the coordination sphere is of the octahedral type with linear HFeNCC fragments (Figure 4). Both isomers of **1**++, i.e. *E*-**1**++ ($[\mathrm{HFe}^{\frown}\mathrm{FeH}]^{2+}$ in Scheme 2) and *Z*-**1**++, and *anti*-**2**++ have planar HFeNCCCCNFeH fragments, while for *syn*-**2**++ the CCCC torsion angle is −81.5°. For each particular structure, both $\{FeH(PH_3)_4NCC\}$ moieties have the same structural parameters and effective atomic charges. The central C−C bond lengths of *E*-**1**++ and *Z*-**1**++ correspond to a C═C bond, whereas for *anti*-**2**++ and *syn*-**2**++ they represent a single C−C bond. The other C−C bonds are shorter for **1**++ than for **2**++ due to π-conjugation for the former case.

The *E*-**1**++ and *anti*-**2**++ isomers are more stable (by 5.47−5.94 and 3.36−3.47 kcal/mol, respectively) than the corresponding *Z*-**1**++ and *syn*-**2**++ ones (thus, only the *E*- and *anti*-isomers, as the most stable ones, will be further discussed) what is in accord with the conceivable isolation of such isomers [a single IR ν(N≡C) band]. The calculated vertical ionization potentials (IP) suggest that **1**++ should be oxidized at slightly higher potentials than **2**++, what agrees with the measured ${}^{I}E_{1/2}{}^{ox}$ values for complexes **1a** and **1c**, although there is not necessarily a direct correlation between the calculated data for isolated molecules and the experimental ones measured for their solutions.

The stronger metal−metal communication for the complex with the unsaturated dinitrile bridge can be rationalized in terms of an electronic interaction involving frontier MOs of the bridging ligand. It was shown[23,37] that the comproportionation constant K_c (reaction 3) correlates with the electron density at the "coordination centers in the LUMO of a bridging π-ligand". Our preliminary calculations on the NCCH═CHCN and $NCCH_2CH_2CN$ ligands show that (i) the contribution of AOs of the coordinating N atoms in the LUMO is higher for the former than for the latter dinitrile (32.2 and 26.2%, respectively) and (ii) the LUMO energy for the former ligand is by 3.62 eV lower than for the latter. Moreover, there is an extensive contribution of the bridging ligand orbitals in some of the *occupied* frontier MOs of *E*-**1**++ (104 and 108, Scheme 3), whereas for *anti*-**2**++ the corresponding MOs are mostly centered at the two metal atoms without a significant involvement of orbitals from that ligand. However, the metal−metal interaction in *E*-**1**++ cannot be accounted for by the other higher energy lying occupied MOs, in particular the two degenerated HOMOs (Figure 5) (mainly localized at the hydride ligands) or the next eight MOs which are based on P atoms.

Interpretation of the Mechanism of Anodic Oxidation. (a) Wave I. The HOMOs of *E*-**1**++ and *anti*-**2**++ (Figure 5) represent the bonding combinations of Fe and hydride orbitals, with a predominant contribution of the latter. Hence, their first oxidation should be hydride centered and lead to a weakening (eventual cleavage) of the Fe−H bond. This is confirmed by the full geometry optimization of the most stable *E*-isomer of the *mono-oxidized* complex *trans*-$[\{FeH(PH_3)_4\}_2(\mu\text{-}N{\equiv}C{-}CH{=}CH{-}C{\equiv}N)]^{3+}$ (*E*-**1**+++), which indicates that one of the hydride hydrogens moves away from the respective iron atom to a distance of 6.53 Å in the equilibrium structure, what in fact corresponds to the cleavage of the Fe−H bond. The other Fe−H bond is preserved. A similar behavior is found for *anti*-**2**++. These results agree with the experimental data (Scheme 2).

The full geometry optimization of the *deprotonated* complex *trans*-$[\{FeH(PH_3)_4\}(\mu\text{-}N{\equiv}C{-}CH{=}CH{-}C{\equiv}N)\{Fe(PH_3)_4\}]^{2+}$ (*E*-**3**++, Figure 4, Scheme 2) shows the occurrence of a structural rearrangement of the $\{Fe(PH_3)_4\}^{+}$ moiety, which now exhibits the vacant site in cis position to the bridging ligand. The HOMO of *E*-**3**++ (Figure 5) is ligand bridge centered and thus its oxidation should not result in loss of the second proton, in accord with Scheme 2. The general conformation of the complex is also preserved. The vertical and adiabatic IPs calculated for *E*-**1**++ and *E*-**3**++ (10.94 and 9.79 eV, respectively, for the adiabatic IP) suggest that the former complex should be oxidized at higher potential than the latter one and this is in agreement with the experimental results (E°_5 is marginally lower than E°_1).

The coordinatively unsaturated *E*-**3**+++ (as well as *E*-**4**+++ formed at wave II) is expected (Scheme 2) to undergo nucleophilic attack, in particular by BF_4^- as is known[9] in the oxidation of the isocyanide complexes *trans*-$[FeH(CNR)(dppe)_2][BF_4]$. The calculations on the model $[Fe(NCCH_3)(PH_3)_4]^{2+}$ **5**++ allowed the location of two minima corresponding to the trans- and cis-isomers (*trans*-**5**++ and *cis*-**5**++, Figure 4), the latter being more stable than the former by 0.09 eV, what correlates with the above isomerization in the oxidation of *E*-**1**++. The theoretical examination of the nucleophilic addition of BF_4^- to *trans*-**5**++ and *cis*-**5**++**,** and the search of the potential surface for these systems indicate that it should proceed without overcoming a potential barrier. The calculations at both HF and CPCM-HF levels (for the latter case the solvent effect was taken into account) showed the formation of *trans*- or *cis*-$[Fe(\eta^1\text{-}FBF_3)(NCCH_3)(PH_3)_4]^{+}$ (*trans*-**6**+ or *cis*-**6**+, Figure 4) with weak bonds between the coordinated F and both Fe and B atoms. For the real solution, the cleavage of the $F_3B{\cdots}F$ bond in **6**+ may well occur to give a fluorinated complex and the solvated BF_3.

(b) Wave II. The overall two-electron oxidation can be considered to correspond to the removal of both electrons from the HOMO of *E*-**1**++ (Figure 5). Thus it should result in weakening of both Fe−H bonds what is confirmed by

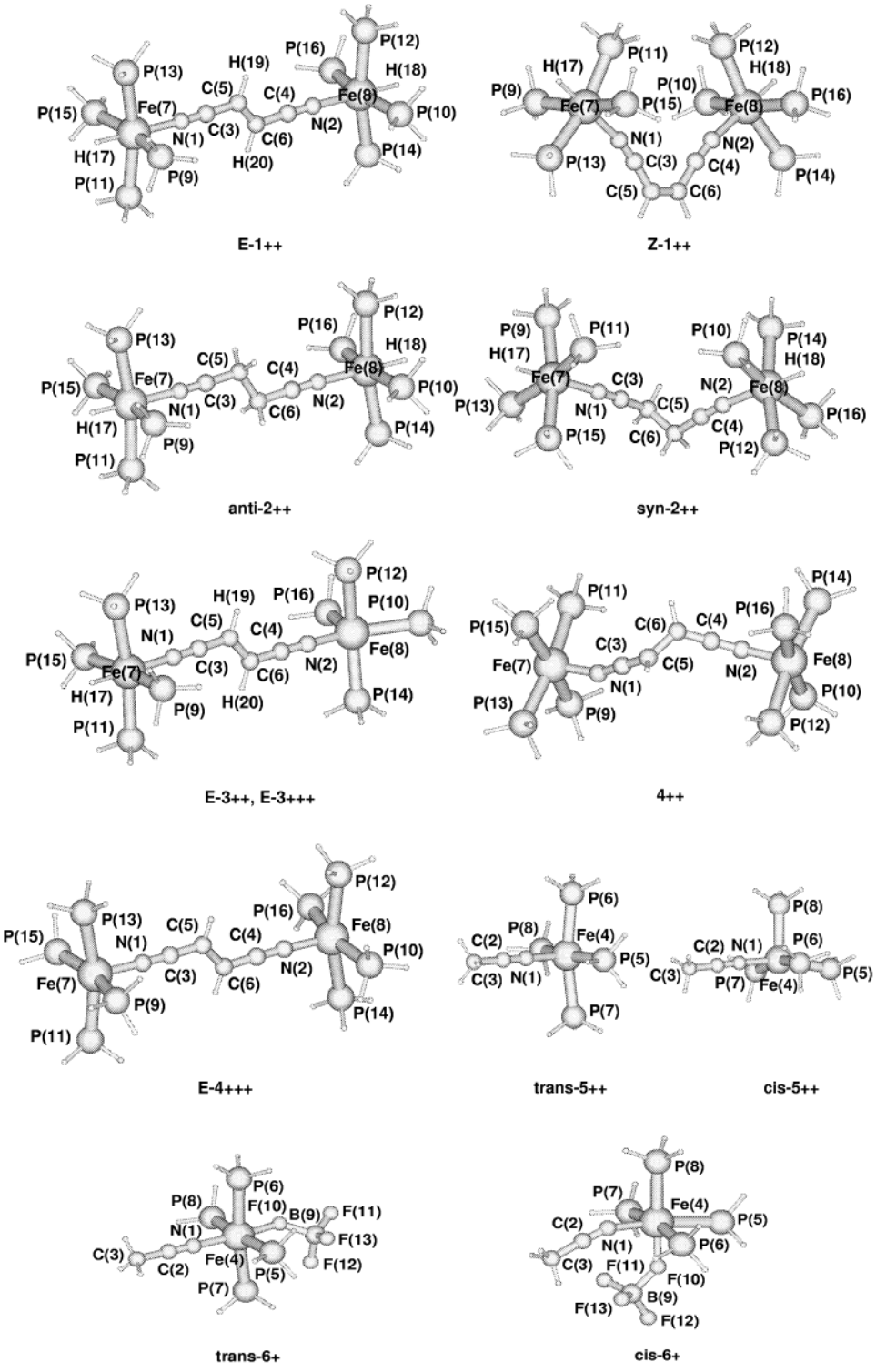

Figure 4. General view of the equilibrium geometries of the calculated structures.

the geometry optimization of *E*-**1**++++′ (with the same structure as the parent *E*-**1**++) which shows a significant elongation of the Fe−H bonds, consistent with the proposed deprotonation (Scheme 2).

Final Remarks

Single-electron oxidation of a metal−hydride center, as shown in this work, constitutes a simple mode of activation of the M−H bond toward heterolytic cleavage (upon increase of the Brönsted acidity) with proton loss that corresponds (the electrons of the bond are transferred to the metal) to a reductive elimination reaction which thus is triggered by an oxidation. This EC-type process can be represented as follows: $M(d^n)-H - e \rightarrow [M(d^{n-1})-H]^+ \rightarrow M(d^{n+1}) + H^+$.

The oxidation can promote not only proton-transfer reactions but also the generation of a reactive coordinatively

Scheme 3. MO Diagrams for the Interaction of the $\{HFe(PH_3)_4\}^+$ Fragment (a) with $\{N{\equiv}CCH{=}CHC{\equiv}N\}$ To Give *E*-**1**++ and (b) with $\{N{\equiv}CCH_2CH_2C{\equiv}N\}$ To Give *anti*-**2**++

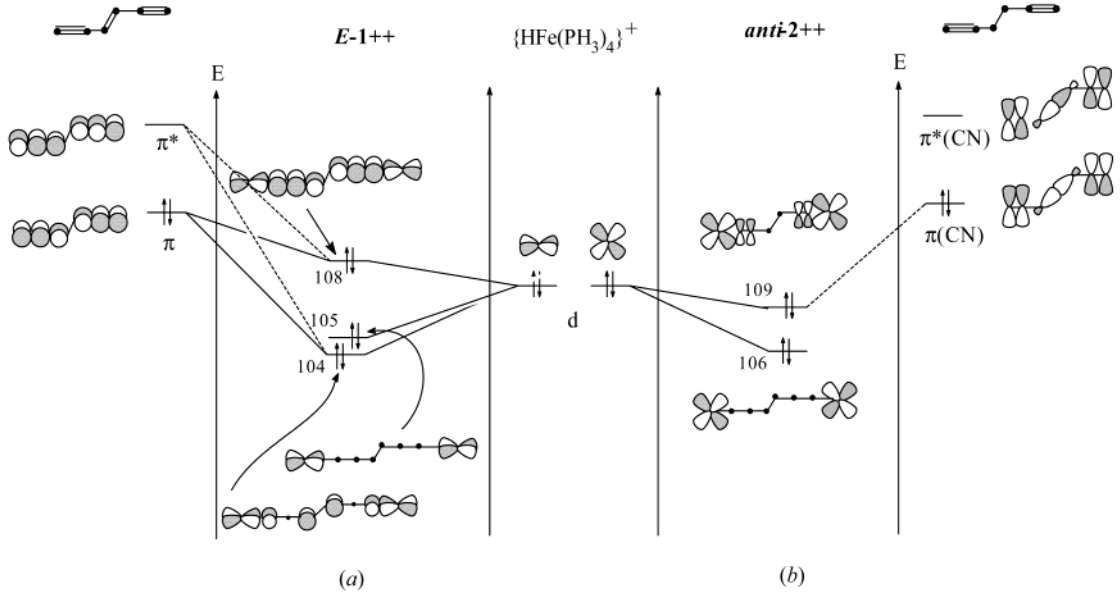

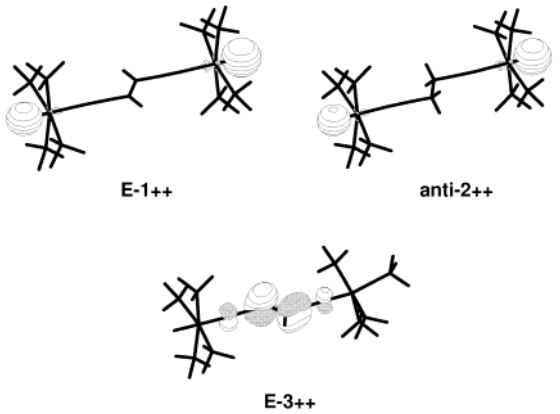

Figure 5. Plots of the HOMOs of *E*-**1**++, *anti*-**2**++, and *E*-**3**++. Only one HOMO for the pair of degenerate ones (for *E*-**1**++ and *anti*-**2**++) is shown.

unsaturated and reduced metal center (with the metal in an unusual oxidation state) which is prone to undergo further ET (e.g. being oxidized at a potential that is not higher than that of the starting hydride complex) or chemical reactions (like addition of a nucleophile). Moreover, if the starting molecule comprises more than one metal−hydride center and these centers communicate electronically in a way that mixed valent complexes with a significant stability are formed, reaction sequences of the above types can occur at distinct oxidation potentials, for instance according to $(EC)^n$ (n = number of M−H centers) processes (as in Scheme 2) or to other E_xC_y combinations, providing a multitude of ET-induced reactions in series of electrogenerated reactive species. Such potentialities are exemplified by this work and deserve further exploration in synthesis.

Theoretical studies can provide a valuable contribution toward the understanding of the various steps involved in such complex behaviors and can assist experimental methods, like cyclic voltammetry and digital simulation, for the establishment of mechanistic details.

Acknowledgment. The work has been partially supported by the Fundação para a Ciência e a Tecnologia (FCT) and by the PRAXIS XXI and POCTI Programs. A. I. F. V. is very grateful to Lic. Sónia Cunha for her great help for teaching how to operate the NMR spectrometer as well as in preliminary electrochemical assays. We also thank Dr. C. Nervi (University of Torino) for making available the electrochemical simulation program, Dr. M. Cândida Vaz (Instituto Superior Técnico) for the elemental analysis services and Mr. Indalécio Marques (Centro de Química Estrutural) for running the FAB-MS spectra.

Supporting Information Available: Table listing selected bond lengths for the calculated structures and plots of selected MOs of *E*-**1**++, *anti*-**2**++, and *E*-**3**++. This material is available free of charge via the Internet at http://pubs.acs.org.

IC025835K